Covalent Attachment of Alkyl Functionality to 50 nm Silicon Nanowires through a Chlorination/Alkylation Process

Muhammad Y. Bashouti,[†] Thomas Stelzner,[‡] Silke Christiansen,[‡,§] and Hossam Haick*[,†]

The Department of Chemical Engineering and Russell Berrie Nanotechnology Institute, Technion, Israel Institute of Technology, Haifa 32000, Israel, Institute of Photonic Technology e.V., Albert-Einstein-Strasse 9, 07745 Jena, Germany, and Max-Planck-Institute of Mikrostructure Physics, Weinberg 2, 06120 Halle, Germany

Received: June 9, 2009

For many applications, the presence of oxide on Si nanowires (Si NWs) is undesirable because of the difficulty in controlling the SiO_2/Si interface properties. Here, we report on the functionalization of 50 nm (in diameter) Si NWs with alkyl chains using a versatile two step chlorination/alkylation process, while preserving the original length and diameter of the NWs. We show that Si NWs terminated with C_1-C_{10} molecules, through Si−C bonds, connect alkyl molecules to 50−100% of the Si atop sites and provide surface stability that depends on the chain length and molecular coverage. These observation were explained by noting that the longer the alkyl chain the higher the concentration of molecule-free pinholes on the Si NW surfaces and, therefore, the easier the oxidation process. Our results provide evidence that alkyl-Si NWs provide stronger Si−C bonds and higher surface stability in ambient conditions than equivalent two-dimensional (2D) Si surfaces having similar or higher initial coverage. The kinetic mechanism of the alkylation process of Si NW surfaces, the oxidation resistance of the modified structures, and the differences from 2D surfaces are discussed in the article.

1. Introduction

The ability to manipulate the properties of silicon nanowires (Si NWs) through controlling their surfaces is important for the realization of Si NW-based devices in the fields of electronics and (bio)sensors.[1–5] A large body of chemistry has been developed for linking moieties chemically to oxidized Si NW surfaces, generally through −OH chemistry, and many pertinent applications have been illustrated.[3,6,7] In other experimental settings/applications, however, the presence of oxide at the Si NW surfaces is undesirable because a defective oxide layer (e.g., native SiO_2) is thought to induce uncontrolled interface states in the silicon.[8–10] Therefore, the surface properties of the (one-dimensional (1D)) nanowires (where zero-dimensional (0D) dots,[11,12] especially those smaller than 3 nm, can be considered as 1D in structure with similar diameter and length) are of far great importance in controlling their electron transport properties.[13–15]

Etching the oxide layer and terminating the Si NW surfaces with hydrogen groups exhibit low surface recombination velocities.[10,16,17] However, these surfaces tend to oxidize within few minutes upon exposure to ambient air. For these surfaces, the more oxide on Si NW surfaces, the higher the density of electrically active trap sites, leading to higher surface recombination velocities of the charge carrier.[10] Hence, there is a considerable interest in learning how to control surface properties through chemical methods. These protection strategies should prevent extensive oxidation of the Si NW surfaces while preserving the low surface recombination velocity of, for example, the H-terminated Si NW surfaces.

Studies with two-dimensional (2D) substrates teach us that adsorption of organic molecules to the Si surface through Si−C bonds[18–24] display a lower rate of oxidation and electron−hole recombination than did unalkylated, H-terminated, or Cl-terminated Si surfaces.[25] To this end, the H-terminated Si surfaces of both single-crystal and porous Si substrates have been alkylated using alkylmagnesium reagents,[5,26–28] and halogenated surfaces have been alkylated using alkylmagnesium or alkyllithium reagents.[29] Alkylation has also been accomplished through free-radical initiation methods such as irradiating with ultraviolet light,[30,31] chemical free-radical activation,[32,33] thermal activation,[34,35] Lewis acid catalyzed hydrosilylation,[36,37] or visible-light-initiated modification of H−Si at room temperature.[38,39] Other methods involve the formation of dangling Si surface bonds using scanning tunneling microscopy (STM) techniques[40] or transition metal-catalyzed reduction of a terminal alkene directly on the Si−H surface.[41,42] Additionally, several electrochemical functionalization methods have been described.[43,44] However, these reactions may lead to significant amounts of oxygen on the surface unless extraordinary measures are taken.[45] This unwanted oxidation reaction is the likely source of electrically active defects observed in electrical measurements of arrays of metal−insulator−semiconductor diodes,[46–49] including cases where low levels of oxide are not detectable via surface analysis techniques (e.g., XPS or FTIR).[50]

In contrast to the 2D Si surfaces, little is known about the chemistry of nonoxidized Si NWs,[51] and even less is known about the correlation between chemical modifications of nonoxidized Si NWs and the electrical and chemical properties of the structures obtained. In this study, we report on the functionalization of Si NW surfaces with C_1-C_{10} alkyl chains using a two step chlorination/alkylation process. Preliminary report on our study can be found in ref 52. The kinetic mechanism of the alkylation process of Si NW surfaces, the oxidation resistance of the modified structures, and the differences from 2D surfaces are discussed in detail.

* To whom correspondence should be addressed. Fax: +972-4-8295672. E-mail: hhossam@technion.ac.il.
[†] Israel Institute of Technology.
[‡] Institute of Photonic Technology e.V.
[§] Max-Planck-Institute of Mikrostructure Physics.

10.1021/jp905394w CCC: $40.75
Published on Web 07/14/2009

2. Experimental Section

The synthesis of the Si NWs (50 ± 10 nm in diameter and 2−4 ± 0.1 μm in length)[52,53] as well as the alkylation process of Si NWs and equivalent 2D Si(100) surfaces through Si−C bonds[52] has been described earlier. For sake of clear presentation, we assign the $\mathbf{C}_n\mathbf{H}_{2n+1}$ (where $n = 1-10$) by $\mathbf{C}_n$.

The chemical composition of the functionalized surfaces was investigated with Thermo VG Scientific (Sigma probe, England) X-ray photoelectron spectroscopy (XPS), equipped with a monochromatized X-ray Al Kα (1486.6 eV) source and operated at a base pressure of $<3 \times 10^{-9}$ torr. Full details about these measurements could be found in our previous preliminary report.[52] In this context, it should be noted that the *inhomogeneous* directionality of the grown Si NWs make the collected spectra insensitive to the angle of the XPS beam. Therefore, analyzing a given Si NW sample at different incident angles gave almost the same peak spectrum. The XPS data from both Si NW and 2D Si(100) are collected from 2.5−3 λ_{Si} (where λ_{Si} = 3.2−3.6 Å stands for the electron escape depth),[54,55] namely, 8−11 Å from the surface. Therefore, the comparison between these two samples is rational. This finding was supported by time-of-flight secondary ion mass spectroscopy (ToF SIMS), as indicated in Results.

The spectra of Si NWs and 2D Si(100) terminated with C_1, C_3, and C_8 alkyl groups, as representative samples, were recorded with a ToF·SIMS5 system (ION-TOF GmbH) in the positive (and negative) mode. A 25 keV, 1pA, 209 Bi^{1+} pulsed primary beam was rastered over a 500 × 500 μm^2 area, and the total primary ion dose was kept well below the static limit (<1012 ions·cm^{-2}). No charge compensation was required. The mass resolution for the characteristic fragments studied ($SiCH_3^+$, $SiC_3H_7^+$, $SiC_8H_{17}^+$, CH_3^-, $C_3H_7^-$, and $C_8H_{17}^-$) was above 9000. The normalization to the spectrum total ion intensity was added for both positive and negative modes.

3. Results

Because of the high silane partial pressure or oxygen residues on the sample surface, the Si NWs grew along one of the ⟨111⟩ directions as well as along other low index growth directions, such as different ⟨112⟩ or ⟨110⟩ directions.[56] The Si NWs with low index surface (100) were the majority.[53] Note: The surface energy, γ, of Si NWs is inversely proportional to the surface atomic densities of the facet. On the basis of this fact, it comes out that $\gamma(100) > \gamma(110) > \gamma(111)$; cf. ref 57.

XPS scans for Si NWs were employed and compared to that of 2D Si(100).[52] To determine the position/shift of the peaks, we have considered two main approaches: (I) the center-to-center distances were fixed at 1.10 ± 0.10 eV between the C-Si and the C-C emissions and at 2.60 ± 0.10 eV between the C-O and the C-Si emissions; and (II) the center-to-center distance allowed flowing, while the full width at half-maximum (fwhm) was identical in Si NW and 2D Si(100) samples. XPS scans for Si NWs showed similar fwhm's for a Si−C bond compared to that of 2D Si(100).[58] In contrast, the Si2p XPS scan for Si NWs showed larger (0.15−0.20 eV) fwhm's than for 2D Si. These fwhm differences in the Si2p core-level components can be attributed to a single effect or a combination of the following effects, which were previously concluded for nanocrystalline systems: (I) structural disorder in the Si;[59,60] (II) phonon broadening;[61,62] and/or (III) shortening the core-hole lifetime between the bulk and atop Si.[63]

Figure 1S of the Supporting Information shows the three main emission regions of C1s XPS spectra of the various molecule-terminated Si NWs: C-Si around 284.22 ± 0.01 eV, C-C around 285.32 ± 0.02 eV, and C-O around 286.67 ± 0.02 eV. Of these peaks, the C-Si peaks can be attributed to molecules bonded *chemically* to the Si surface. In contrast, the C-O peaks can be attributed to adventitious carbonaceous materials that are *physisorbed* on top of the monolayer.[52,64,65] The emission at 285.20 ± 0.02 eV can be ascribed to adventitious C-C or C-H specimen that do not participate in the Si-C bond.

TABLE 1: Summary of the Γ_{sat} Results for Alkyl Chains Bonded to Si NW Surfaces via Si−C Bonds

sample	Γ_{sat}[a] (min)	C-Si/Si2p ratio
C_1-Si NW[b]	20 ± 2	0.135 ± 0.001
C_2-Si NW[b]	50 ± 10	0.093 ± 0.003
C_3-Si NW[b]	60 ± 10	0.075 ± 0.006
C_4-Si NW[b]	65 ± 10	0.066 ± 0.004
C_5-Si NW[b]	90 ± 10	0.068 ± 0.012
C_6-Si NW[b]	120 ± 10	0.076 ± 0.009
C_8-Si NW	450 ± 20	0.073 ± 0.002
C_9-Si NW	1000 ± 50	0.104 ± 0.003
C_{10}-Si NW	1000 ± 50	0.077 ± 0.003

[a] Γ_{sat} is the time required to achieve 92 ± 3% of the saturation level of the adsorption curve. [b] These data were originally reported in ref 52, but we reproduce them in the current table for the convenience of the reader.

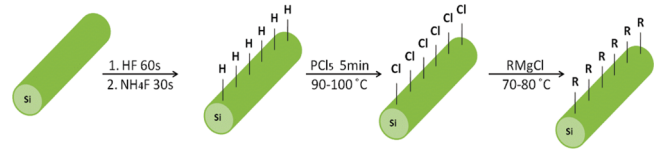

Figure 1. Si NW functionalization scheme for the two step chlorination/alkylation process.

For analyzing the collected XPS spectra, the integrated area under the C-Si peak was divided by the integrated area under the Si2p peak and normalized by scan time. The alkylation rate of the short alkyl chains (C_1-C_6)[52] at alkylation processes <100 min was higher than those for long alkyl chains (C_8-C_{10}). The times required to achieve 92 ± 3% of the saturation level of the various adsorption curves, Γ_{sat}, together with the related C-Si/Si2p ratios, are summarized in Table 1. Longer alkylation times, up to 24 h, changed the total coverage by only 5 ± 3%. Alkylation times of 24−72 h did not further change the coverage on Si NWs and 2D Si(100). The highest coverage of a specific alkyl functionally (hereafter, $(C\text{-}Si/Si2p)_{max\text{-}alkyl}$) was compared with the highest coverage obtained for C_1 functionality (hereafter, $(C\text{-}Si/Si2p)_{max\text{-}C1}$). This comparison is expressed throughout the text as $\Gamma_{max\text{-}alkyl} = (C\text{-}Si/Si2p)_{max\text{-}alkyl}/(C\text{-}Si/Si2p)_{max\text{-}C1}$. Figure 2 shows the $\Gamma_{max\text{-}alkyl}$ on Si NWs and 2D Si(100) as a function of the alkyl chain length.[66] The figure shows that the C_1 functionality in both Si NWs and 2D Si(100) gave the highest coverage values. Increasing the chain length by one carbon gave $\Gamma_{max\text{-}C2} = 70 \pm 5\%$ on Si NWs and $\Gamma_{max\text{-}C2} = 60 \pm 20\%$ on 2D Si(100), indicating that the C_2 functionality can be packed at a high density without major steric effects. Increasing the alkyl chain to C_3 gave $\Gamma_{max\text{-}C3} = 55 \pm 5\%$ on Si NWs and $\Gamma_{max\text{-}C3} = 35 \pm 2\%$ on 2D Si(100). In the C_3-C_5 region, increasing the chain length decreased the $\Gamma_{max\text{-}alkyl}$ from 55 ± 5% to 50 ± 5% on Si NWs and maintained it constant (35 ± 2%) on 2D Si(100) surfaces. In the C_6-C_{10} region, increasing the chain length increased the $\Gamma_{max\text{-}alkyl}$ gradually from 50 ± 10% to 60−76 ± 4% on Si NWs and maintained it as almost constant (35−40 ± 10%) on 2D Si(100) surfaces.

ToF SIMS experiments were carried out representatively on C_1-Si NWs, C_3-Si NWs, and C_8-Si NWs, and, for comparison, on 2D C_1-Si(100), 2D C_3-Si(100), and 2D C_8-Si(100) samples.

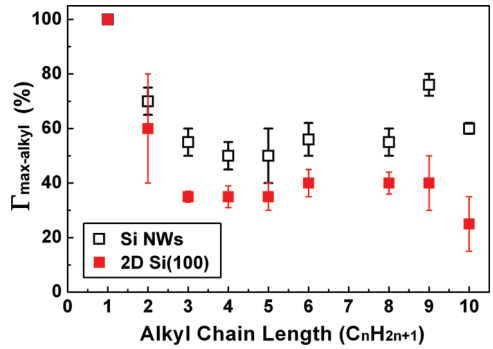

Figure 2. $\Gamma_{max\text{-}alkyl}$ versus alkyl chain length on Si NWs and, for comparison, on 2D Si(100) surfaces. Note: $\Gamma_{max\text{-}alkyl} = (C\text{-}Si/Si2p)_{max\text{-}alkyl}/(C\text{-}Si/Si2p)_{max\text{-}C1}$.

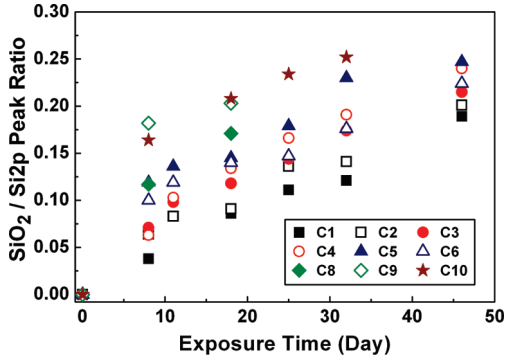

Figure 3. Observed oxidation (SiO_2/Si2p peak ratio) at different exposure times to ambient air.[67]

For these surfaces, the alkyl coverage is proportional to the $SiCH_3^+$ (or CH_3^-), $SiC_3H_7^+$ (or $C_3H_7^-$), and $SiC_8H_{17}^+$ (or $C_8H_{17}^-$) ToF SIMS fragments from C_1-Si, C_3-Si, and C_8-Si samples, respectively. The difference between the ToF-SIMS-based $\Gamma_{max\text{-}alkyl}$ on Si NWs and 2D Si(100) was found to be ~0 ± 3% for C_1-Si, ~17 ± 4% for C_3-Si, and ~22 ± 4% for C_8-Si samples, in a good agreement with the XPS results presented in Figure 2.

The samples were exposed to ambient air for several weeks to investigate the stability of the alkylated Si NWs (Figure 3 and Table 2).[67] The degree of observed oxidation of alkyl-Si NWs was extracted from the ratio between the integrated area under the SiO_2 peak (103.50 ± 0.02 eV) and the Si2p peaks. For a specific alkyl molecule, the oxide grew monotonically with the exposure time. On all alkylated Si NWs, SiO_2 growth was negligible for the first 2 to 3 days of the experiment but began to be considerable after 8 days in air. For all alkyl molecules, the Si NWs exhibited significantly higher stability against oxidation than 2D Si(100). After 8 days of exposure to air, Si NWs and 2D Si(100) surfaces showed SiO_2/Si2p ratios of 0.04−0.11 and 0.15−0.18, respectively. The (0.15−0.18) value obtained for 2D Si(100) surfaces after 8 days of exposure to air was similar to that of Si NWs after 42 days.[67]

Comparison between the data presented in Figure 2 and Figure 3 and Table 2 showed (in general) that the higher the surface coverage the higher the oxidation resistance and vice versa. For example, after 10 days of exposure to air, C_1-Si NWs showed a 2-fold higher oxidation resistance than that of C_6-Si NWs. Different alkyl molecules having similar $\Gamma_{max\text{-}alkyl}$ values showed different oxidation resistances. For example, after 8 days of exposure to air, C_2-Si NWs showed 3−4-fold higher oxidation resistance than C_9-Si NWs. Similar behavior was observed in C_4-Si NWs, C_5-Si NWs, and C_{10}-Si NWs, all of which have $\Gamma_{max\text{-}alkyl}$ of ~55%. Surprisingly, C_1-Si NWs exposed to air over a period of more than a month showed approximately three times less oxidation than the 2D C_1-Si(100) surfaces, although both surfaces initially have similar $\Gamma_{max\text{-}C1}$ values. These discrepancies in oxidation resistance are discussed in section 4.4.

4. Discussion

4.1. Reaction Kinetics. The dependence of the reaction constant at short alkylation times (hereafter, k_{p1}) on the length of alkyl chains could be attributed to a weighted contribution of the nucleophile attack and the intersteric effect during the alkylation process. The determination of parameters k_{p1} and k_{p2} depends on the starting point of the propagation step (Si-Cl $\xrightarrow{\text{R-MgCl}}$ Si-R). In this step, three processes take place in parallel (the so-called transition state; see Figure 4). At first, the nucleophilic carbons attack electron deficient electrophilic centers (atoms of atop Si) and bond to them, expelling other groups (Cl). The incoming group will then replace the expelled group, as illustrated in Figure 4. The addition of the nucleophile and the elimination of the expelled group take place simultaneously and determine the reaction's rate step. This slow, rate-determining step process is termed bimolecular nucleophilic substitution (or S_N2) and exhibits a second-order reaction rate because it depends on the concentration of the nucleophile (R-MgCl; see Figure 4, path 1) and Cl-terminated Si sites (see Figure 4, path 2). In this scenario, the alkylation rate can be expressed as:

$$\frac{1}{\text{rate}} = \frac{1}{k_{p1}[\text{alkyl}][\text{Si-Cl}]} \quad (1)$$

where k_{p1} stands for pseudofirst-order rate constant of the reaction. Abstraction of $[MgCl]^+$ by Cl^- (Figure 4, path 3) plays no role in determining the reaction rate. From Figure 5, it is easy to see that the longer the alkyl chain the lower the reaction constant at short alkylation times (hereafter, k_{P1}). For example, k_{P1} of the methyl (C1) group (2.64×10^{-2} min^{-1}) was 38 times larger than k_{p1} of the decane (C10) group (7.0×10^{-4} min^{-1}).

As the molecule becomes longer, the alkyl chain punches more net negative charge on the anionic carbon in the alkyl Grignard (R-MgCl), viz. on the carbon near the Mg atom. However, when the molecule becomes longer, it folds, rotates, and vibrates in all directions. This phenomenon makes the molecule less reactive and, as a result, limits the nucleophilic attack. For short molecules, the twisting is negligible, as compared to long molecules, leading to fast nucleophilic attack and fast reaction rates.

In the region between Γ_{sat} and maximum coverage of alkyl functionality, a significant fraction of the available atop sites are surrounded by occupied alkylated sites and are difficult to assess. In these conditions, the intersteric effects become more relevant than the nucleophilic attack, and the reaction switches to zero-order, which characterized by a reaction rate k_{p2}.[68] To demonstrate the change of driving force from nucleophile attack to steric-effect, we plot the k_{p1}/k_{p2} ratio as a function of the chain length (Figure 5). The results of this plot show a first order exponential decay in the following form:

$$\frac{k_{P1}}{k_{P2}} = A \times \exp\left(-\frac{C_1 - C_n}{2}\right) \quad (2)$$

TABLE 2: Summary of the Observed Oxidation (SiO_2/Si2p Peak Ratio) of the Various Molecule-Terminated Si NW Samples, as Presented in Figure 3, at Different Exposure Times to Ambient Air[67]

exposure time (days)	C1	C2	C3	C4	C5	C6	C8	C9	C10
0	0.00 ± 0.01	0.00 ± 0.02	0.00 ± 0.02	0.00 ± 0.02	0.00 ± 0.02	0.00 ± 0.02	0.00 ± 0.02	0.00 ± 0.02	0.00 ± 0.02
8	0.04 ± 0.01	0.06 ± 0.02	0.07 ± 0.02	0.06 ± 0.02	0.12 ± 0.02	0.10 ± 0.02	0.12 ± 0.03	0.18 ± 0.04	0.16 ± 0.04
11	0.08 ± 0.02	0.08 ± 0.02	0.10 ± 0.01	0.10 ± 0.02	0.14 ± 0.01	0.12 ± 0.03			
18	0.09 ± 0.02	0.09 ± 0.03	0.12 ± 0.02	0.13 ± 0.02	0.15 ± 0.02	0.14 ± 0.02	0.17 ± 0.03	0.20 ± 0.04	0.21 ± 0.04
25	0.11 ± 0.03	0.14 ± 0.02	0.14 ± 0.03	0.17 ± 0.03	0.18 ± 0.02	0.15 ± 0.02			0.23 ± 0.05
32	0.12 ± 0.02	0.14 ± 0.02	0.17 ± 0.02	0.19 ± 0.02	0.21 ± 0.03	0.18 ± 0.03			0.25 ± 0.04
46	0.19 ± 0.02	0.20 ± 0.04	0.22 ± 0.03	0.24 ± 0.03	0.25 ± 0.03	0.22 ± 0.02			

TABLE 3: $SiC_xH_y^+$ Peak Intensities of ToF-SIMS Spectra of C_1-Si NWs and 2D C_1-Si(100) Surfaces before and after 4 Days of Exposure to an Oxidizing Atmosphere

	oxidation time C_1-Si NWs		oxidation time 2D C_1-Si(100)	
segment	0 days	4 days	0 days	4 days
Si-O	0.037 ± 0.002	0.063 ± 0.003	0.021 ± 0.001	0.039 ± 0.001
Si-C	0.142 ± 0.006	0.091 ± 0.009	0.074 ± 0.001	0.039 ± 0.001
Si-CH_3	0.239 ± 0.011	0.202 ± 0.013	0.382 ± 0.041	0.301 ± 0.010
$Si_2OC_2H_6$	0.004 ± 0.001	0.008 ± 0.001	0.004 ± 0.0002	0.003 ± 0.0002
Si_2O	0.071 ± 0.002	0.139 ± 0.002	0.030 ± 0.0005	0.066 ± 0.0003

where C_1 is the carbon number of the methyl group (=1), C_n is the carbon number of alkyl chains having $n = 2-11$, A is a dimensionless constant that represents the kinetic ratio when $n = 1$. The exponential decay in eq 2 indicates that the steric effect increases exponentially with increasing molecule length. For $n > 11$, k_{p1} becomes comparable to k_{p2}, thus indicating that the steric effect in long molecules becomes the main driving force not only in the late stages of the reaction process but also in the early propagation reaction time.

4.2. Effect of Chain Length of Alkyl Molecules. According to theoretical simulations, steric effects (van der Waals diameter) can hinder formation of dense alkyl packing of straight-chain groups that are longer than C_1. Indeed, increasing the length of the alkyl chain increases the van der Waals diameter from 2.5 Å (in the case of C_1) to >4.5−5.0 Å for longer alkyl chains. The latter van der Waals diameters are much larger than the internuclear distance between adjacent Si atoms (3.8 Å), a matter that decreases their adsorption rate and limits their coverage to maximum 50−55% of a monolayer of Si surface sites.[32]

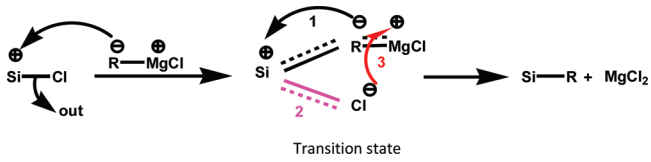

Figure 4. At the transition state, an alkyl molecule adds to the chlorine silicon. Three processes are occurring in parallel. First, the anionic carbon abstracts (i.e., *nucleophilic* carbon attack) the silicon atom to generate the Si−C bond. Second, the Si−Cl bond is degenerated. The degenerated Cl atom (from the Si−Cl bond) abstracts the Mg atom.

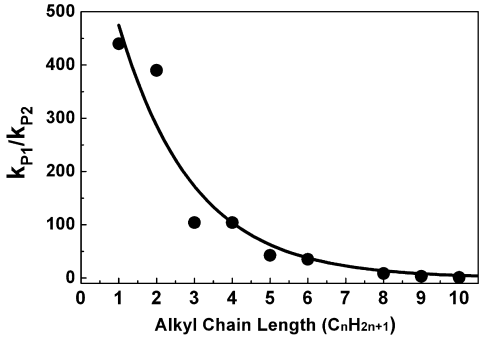

Figure 5. First order exponential decay of k_{P1}/k_{P2} ratio as a function of alkyl chain length.

With these findings in mind, we found the chain length dependence in Figure 2 to be consistent with the similar decay of the coverage reported by others on flat Si(111) surfaces for longer chains than in the present work, with, however, no increase of coverage above 7 carbon atoms (cf. ref 69). Basically, these discrepancies call claim that the higher coverage obtained for $>C_6$ chain lengths in the present study might be artificial and/or not significant due to fitting problems of the XPS data (cf. ref 69). In contrast, few experimental observations suggest that the coverage behavior of $>C_6$ chain lengths on Si NWs might not be artificial, as justified in the following:

(1) ToF SIMS experiments (which, basically, eliminate potential artificial observations) have shown higher absolute coverage in the case of $>C_6$ chain lengths, in good consistency with XPS observations.
(2) In the case of 2D Si(100) surface, the results of ToF SIMS have shown (more or less) the expected coverage versus chain length behavior; at the time, similar behavior was not observed in the case of Si NWs.
(3) The experimental error and/or accuracy of the peak fitting are relatively small (4−11%).

It is reasonable that passivation of Si NWs by alkyl molecules is determined by a balance of two main factors:[70] (I) molecule−molecule lateral interaction and (II) molecule−substrate vertical interaction. For short alkyl chains (C_1-C_5), which exhibit liquid-like behavior and thermal fluctuations,[71,72] the determining factor of the alkylation process is molecule−substrate interaction. Increasing the chain length to C_6-C_{10} forms a solid-like phase, where the molecule−molecule lateral interactions become more dominant in determining the coverage outcome of the Si NW surface. It is worth pointing out in this context that lateral interactions between long alkyl chains might be formed during the *physisorption* (or solvent) stage, before the covalent bonding between the carbon and silicon atoms (i.e., *chemisorption*) is completed.[73,74]

4.3. Oxidation Resistance of Si NWs. On the basis of the results presented in Figures 2 and Figure 3 and Table 2, it is easy to see that the longer the alkyl chain the lower the oxidation resistance of the Si NW surfaces, regardless of the $\Gamma_{max\text{-}alkyl}$ values of the various alkyl-Si NWs.[67] This observation could

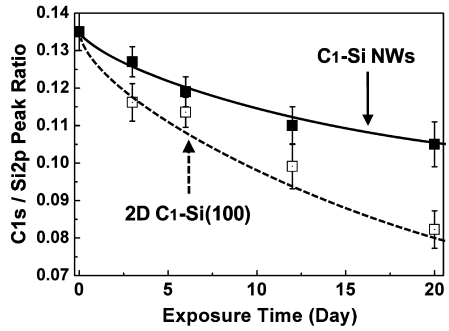

Figure 6. Decay of C-Si XPS signal as a function of exposure time for C_1-Si NW and 2D C_1-Si(100).

be explained by noting that the attractive interactions between the adjacent molecular chains increase by 4.6 kJ/mol per methylene unit.[75–77] In this case, the longer the alkyl chain, the higher the probability for the formation of molecular domains (or islands) separated by (nanometric) molecule-free pinholes[78] and, consequently, the higher accessibility of oxidizing species to the bare (molecule-free) surfaces of the Si NWs.

4.4. Differences between Alkyl-Terminated Si NWs and 2D Si(100). The exceedingly higher diameters (50 ± 10 nm) of Si NWs than the length of the alkyl molecules (0.2−1.6 ± 0.1 nm) point out the marginal gain in steric hindrance between adsorbed alkyl molecules on Si NW surfaces (cf. refs 79 and 80). This fact calls claim that the observed differences between alkyl-Si NWs and 2D alkyl-Si(100) surfaces are related to different surface energies[57] and/or strengths of Si−C bonds.

The higher oxidation resistance of alkyl-Si NW surfaces, compared to 2D alkyl-Si(100) surfaces, can be attributed to the formation of stronger Si−C bonds between the alkyl functionalities and Si NW surfaces. Step forward analysis results of a C_1-Si NW, as a representative sample, showed 22% decrease in the Si−C bond signal after 20 days; at the time, the 2D C_1-Si(100) samples showed >34% decrease of the same signal (see Figure 6). To understand these observations, ToF SIMS fragments of C_1-Si NWs and 2D C_1-Si(100) surfaces were collected at different exposure periods to oxidizing agents. Table 3 presents selected ToF SIMS spectrum peaks of the C_1-Si NW before and after 4 days exposure to a pure (>99.9999% purity) O_2(20%)/N_2(80%) environment containing 10−15% RH. As shown in the table, after 4 days of oxidation the Si_xO signal (where $x = 1,2$) of Si NW samples increased by 70−95 ± 10%, while the concentration of Si−C and Si−CH_3 bonds decreased by 36 ± 2% and 15 ± 2%, respectively. The higher (absolute) changes in the Si_xO signal suggest that the molecule-free Si−Si bonds are easier to break upon interaction with O_2 and/or H_2O molecules than the Si−C bonds. The higher change in the Si−C (36 ± 2%) signal than that in Si-CH_3 (15 ± 2%) indicates that the Si−C bond is more easy for oxidation than the Si−Si bond directly beneath the −CH_3 group. These results indicate that the Si−Si back-bonds are broken first to form Si−O−Si back-bonds. After all Si−Si back-bonds are oxidized, the oxidizing species will start attacking the Si−C bonds. For 2D C_1-Si(100) surfaces, the Si_xO signal (where $x = 1,2$) increased by 86−120 ± 10%, while the concentration of Si−C and Si−CH_3 bonds decreased by 47 ± 2% and 21 ± 2%, respectively, after 4 days of exposure to the oxidizing atmosphere. Comparing the relative changes obtained for 2D C_1-Si(100) surfaces and C_1-Si NWs, one can call for two main conclusions. The first is that C_1-Si NWs are more stable than 2D C_1-Si(100) surfaces, consistent with the XPS observation reported earlier in this article. The second is that the oxidation mechanism of 50 ± 10 nm (in diameter) C_1-Si NWs is similar to that of 2D C_1-Si(100) surfaces.

Summary and Conclusions

A two step chlorination/alkylation process was used to connect C_1−C_{10} alkyl functionality to Si NWs and, for comparison, to 2D Si(100) surfaces. Among all studied alkyl molecules, the C_1 functionality provided the highest coverage on both Si NWs and 2D Si(100). Increasing the chain length from C_1 to C_{10} showed a nonmonotonic correlation with $\Gamma_{max\text{-}alkyl}$ and a minimum coverage at the C_4−C_5 region for Si NWs and at the C_3−C_5 region for 2D Si(100) samples. Exposure of the samples to ambient conditions showed that the longer the alkyl chain the lower the oxidation resistance of the Si NW surfaces, regardless of the $\Gamma_{max\text{-}alkyl}$ values of the various alkyl-Si NWs. This observation was explained by noting that the longer the alkyl chain, the higher the *heterogeneous* adsorption of molecules on the Si NWs, i.e., the higher the probability for the formation of molecular domains separated by (nanometric) molecule-free pinholes. In this case, the higher the concentration of molecule-free pinholes, the easier the oxidation process. Our results provide evidence that Si NWs terminated with alkyl groups provide stronger Si−C bonds and higher surface stability in ambient conditions than equivalent 2D Si surfaces having similar or higher initial coverage. A preliminary mechanism explaining the performance of the Si−C bonds on Si NWs was discussed, but more studies need to target this topic thoroughly.

An important corollary to our findings is that only molecules that cover >70% of the Si atop sites can be well-utilized for chemical passivation of Si NWs. A possible way to achieve this is to utilize alkyl chains longer than C_6 that are *homogenously* adsorbed on the Si NW surface.[79] Alkyl molecules longer than C_1−C_2 but with a straight Si−C bond, such as the propenyl (CH_3−CH═CH−) functionality,[5] can be utilized to form nearly full coverage of Si NWs, thus increasing the oxidation resistance of these surfaces. Our results are of practical importance when oxide free surfaces are required, e.g., for radial epitaxy on NWs to realize vertical P−N junctions for solar cells or radial Si/Ge superlattices for application in optoelectronics.

Acknowledgment. We acknowledge the Marie Curie Excellence Grant of the FP6 (to H.H.) and financial support from the US-Israel Binational Science Foundation (to H.H.), the Russell Berrie Nanotechnology Institute (to H.H.), and the Deutsche Forschungsge-meinschaft (DFG) under contract number CH159/1 (to S.C.), and Ossama Assad and Yair Paska (Technion) for assistance and fruitful discussions. M.Y.B. thanks the Zeff Fellowship for partial support. H.H. holds the Horev Chair for the Leaders in Science and Technology.

Supporting Information Available: C1s XPS spectra for molecule-terminated Si NWs and 2D Si(100) samples, and summary of the C-O/Si2p peak area ratio of the various molecule-terminated Si NW and 2D Si(100) surfaces. This material is available free of charge via the Internet at http://pubs.acs.org.

References and Notes

(1) Jie, J.; Zhang, W.; Peng, K.; Yuan, G.; Lee, C. S.; Lee, S.-T. *Adv. Funct. Mater.* **2008**, *18*, 3251–3257.
(2) Chen, L. J. *J. Mater. Chem.* **2007**, *17*, 4639–4643.
(3) Patolsky, F.; Lieber, C. M. *Mater. Today* **2005**, *8*, 20–28.
(4) Duan, X.; Huang, Y.; Lieber, C. M. *Nano. Lett.* **2002**, *2*, 487–490.
(5) Assad, O.; Puniredd, S. R.; Haick, H. *J. Am. Chem. Soc.* **2008**, *130*, 17670–17671.
(6) Cui, Y.; Wei, Q.; Park, H.; Lieber, C. M. *Science* **2001**, *293*, 1289–1292.
(7) Cui, Y.; Zhong, Z.; Wang, D.; Wang, W. U.; Lieber, C. M. *Nano. Lett.* **2003**, *3*, 149–152.

(8) Aswal, D. K.; Lenfant, S.; Guerin, D.; Yakhmi, J. V.; Vuillaume, D. *Anal. Chim. Acta* **2006**, *568*, 84–108.
(9) Kelzenberg, M. D.; Turner-Evans, D. B.; Kayes, B. M.; Filler, M. A.; Putnam, M. C.; Lewis, N. S.; Atwater, H. A. *Nano Lett.* **2008**, *8*, 710–714.
(10) Haick, H.; Hurley, P. T.; Hochbaum, A. I.; Yang, P.; Lewis, N. S. *J. Am. Chem. Soc.* **2006**, *128*, 8990–8991.
(11) Rosso-Vasic, M.; Spruijt, E.; van Lagen, B.; De Cola, L.; Zuilhof, H. *Small* **2008**, *4*, 1835–1841.
(12) Wolkin, M. V.; Jorne, J.; Fauchet, P. M.; Allan, G.; Delerue, C. *Phys. Rev. Lett.* **1999**, *82*, 197–200.
(13) Yan, H.; Yang, P. *Chem. Nanostruct. Mater.* **2003**, 183–226.
(14) Duan, X.; Huang, Y.; Cui, Y.; Lieber, C. M. *Mol. Nanoelectronics* **2003**, 199–227.
(15) Kamins, T. *Electrochem. Soc. Interface* **2005**, *14*, 46–49.
(16) Ma, D. D. D.; Lee, C. S.; Au, F. C. K.; Tong, S. Y.; Lee, S. T. *Science* **2003**, *299*, 1874–1877.
(17) Sun, X. H.; Wang, S. D.; Wong, N. B.; Ma, D. D. D.; Lee, S. T.; Teo, B. K. *Inorg. Chem.* **2003**, *42*, 2398–2404.
(18) Aswal, D. K.; Lenfant, S.; Guerin, D.; Yakhmi, J. V.; Vuillaume, D. *Anal. Chimi. Acta* **2006**, *568*, 84–108.
(19) Shirahata, N.; Hozumi, A.; Yonezawa, T. *Chem. Rec.* **2005**, *5*, 145–159.
(20) De Smet, L. C. P. M.; Pukin, A. V.; Sun, Q.-Y.; Eves, B. J.; Lopinski, G. P.; Visser, G. M.; Zuilhof, H.; Sudhoelter, E. J. R. *Appl. Surf. Sci.* **2005**, *252*, 24–30.
(21) Lewis, N. S. *Inorg. Chem.* **2005**, *44*, 6900–6911.
(22) Filler, M. A.; Bent, S. F. *Prog. Surf. Sci.* **2003**, *73*, 1–56.
(23) Buriak, J. M. *Chem. Rev.* **2002**, *102*, 1271–1308.
(24) Bent, S. F. *J. Phys. Chem. B* **2002**, *106*, 2830–2842.
(25) Webb, L. J.; Lewis, N. S. *J. Phys. Chem. B* **2003**, *107*, 5404–5412.
(26) Bansal, A.; Li, X.; Lauermann, I.; Yi, S.; Weinberg, W. H.; Lewis, N. S. *J. Am. Chem. Soc.* **1996**, *118*, 7225–7226.
(27) Puniredd, S. R.; Assad, O.; Haick, H. *J. Am. Chem. Soc.* **2008**, *130*, 9184–9185.
(28) Puniredd, S. R.; Assad, O.; Haick, H. *J. Am. Chem. Soc.* **2008**, *130*, 13727–13734.
(29) Bansal, A.; Li, X.; Yi, S. I.; Weinberg, W. H.; Lewis, N. S. *J. Phys. Chem. B* **2001**, *105*, 10266–10277.
(30) Terry, J.; Linford, M. R.; Wigren, C.; Cao, R.; Pianetta, P.; Chidsey, C. E. D. *Appl. Phys. Lett.* **1997**, *71*, 1056–1058.
(31) Effenberger, F.; Gotz, G.; Bidlingmaier, B.; Wezstein, M. *Angew. Chem., Int. Ed.* **1998**, *37*, 2462–2464.
(32) Sieval, A. B.; Linke, R.; Heij, G.; Meijer, G.; Zuilhof, H.; Sudhoelter, E. J. R. *Langmuir* **2001**, *17*, 7554–7559.
(33) Linford, M. R.; Fenter, P.; Eisenberger, P. M.; Chidsey, C. E. D. *J. Am. Chem. Soc.* **1995**, *117*, 3145–3155.
(34) Sieval, A. B.; Demirel, A. L.; Nissink, J. W. M.; Linford, M. R.; van der Maas, J. H.; de Jeu, W. H.; Zuilhof, H.; Sudhoelter, E. J. R. *Langmuir* **1998**, *14*, 1759–1768.
(35) Sung, M. M.; Kluth, G. J.; Yauw, O. W.; Maboudian, R. *Langmuir* **1997**, *13*, 6164–6168.
(36) Boukherroub, R.; Morin, S.; Bensebaa, F.; Wayner, D. D. M. *Langmuir* **1999**, *15*, 3831–3835.
(37) Buriak, J. M.; Stewart, M. P.; Geders, T. W.; Allen, M. J.; Choi, H. C.; Smith, J.; Raftery, D.; Canham, L. T. *J. Am. Chem. Soc.* **1999**, *121*, 11491–11502.
(38) Scheres, L.; Achten, R.; Giesbers, M.; de Smet, L. C. P. M.; Arafat, A.; Sudhoelter, E. J. R.; Marcelis, A. T. M.; Zuilhof, H. *Langmuir* **2008**, *25*, 1529–1533.
(39) Scheres, L.; Arafat, A.; Zuilhof, H. *Langmuir* **2007**, *23*, 8343–8346.
(40) Cicero, R. L.; Chidsey, C. E. D.; Lopinski, G. P.; Wayner, D. D. M.; Wolkow, R. A. *Langmuir* **2002**, *18*, 305–307.
(41) Ciampi, S.; Boecking, T.; Kilian, K. A.; James, M.; Harper, J. B.; Gooding, J. J. *Langmuir* **2007**, *23*, 9320–9329.
(42) Saghatelian, A.; Buriak, J.; Lin, V. S. Y.; Reza Ghadiri, M. *Tetrahedron* **2001**, *57*, 5131–5136.
(43) Allongue, P.; De Villeneuve, C. H.; Pinson, J.; Ozanam, F.; Chazalviel, J. N.; Wallart, X. *Electrochim. Acta* **1998**, *43*, 2791–2798.
(44) Allongue, P.; Henry de Villeneuve, C.; Morin, S.; Boukherroub, R.; Wayner, D. D. M. *Electrochim. Acta* **2000**, *45*, 4591–4598.
(45) Hart, B. R.; Letant, S. E.; Kane, S. R.; Hadi, M. Z.; Shields, S. J.; Reynolds, J. G. *Chem. Comm.* **2003**, *3*, 322–323.
(46) Faber, E. J.; de Smet, L. C. P. M.; Olthuis, W.; Zuilhof, H.; Sudhoelter, E. J. R.; Bergveld, P.; van den Berg, A. *ChemPhysChem* **2005**, *6*, 2153–2166.
(47) Sieval, A. B.; Vleeming, V.; Zuilhof, H.; Sudhoelter, E. J. R. *Langmuir* **1999**, *15*, 8288–8291.
(48) Salomon, A.; Boecking, T.; Gooding, J. J.; Cahen, D. *Nano Lett.* **2006**, *6*, 2873–2876.
(49) Yu, H.-Z.; Boukherroub, R.; Morin, S.; Wayner, D. D. M. *Electrochem. Commun.* **2000**, *2*, 562–566.
(50) Seitz, O.; Boecking, T.; Salomon, A.; Gooding, J. J.; Cahen, D. Langmuir 2006, *16*.
(51) Bunimovich, Y. L.; Shin, Y. S.; Yeo, W. S.; Amori, M.; Kwong, G.; Heath, J. R. *J. Am. Chem. Soc.* **2006**, *128*, 16323–16331.
(52) Bashouti, M. Y.; Stelzner, T.; Berger, A.; Christiansen, S.; Haick, H. *J. Phys. Chem. C* **2008**, *112*, 19168–19172.
(53) Stelzner, T.; Andra, G.; Wendler, E.; Wesch, W.; Scholz, R.; Goesele, U.; Christiansen, S. *Nanotechnology* **2006**, *17*, 2895–2898.
(54) Pi, T. W.; Hong, I. H.; Cheng, C. P.; Wertheim, G. K. *J. Electron Spectrosc. Relat. Phenom.* **2000**, *107*, 163–176.
(55) Himpsel, F. J.; Meyerson, B. S.; McFeeley, F. R.; Morar, J. F.; Taleb-Ibrahimi, A.; Yarmoff, J. A. *1988 Enrico Fermi School on Photoemission and Absorption Spectroscopy of Solids and Interfaces with Synchrotron Radiation, Varenna, North-Holland*: Amsterdam, 1988; p 203−236.
(56) Because of the different facets on Si NW surfaces, Si-H, Si-H_2, and/or Si-H_3 terminations might be formed on the H-terminated Si NW surfaces. However, due to steric constraints of the alkyl molecules, only Si-H terminations can participate in the nucleophilic (or alkylation) reaction.
(57) Zhang, R. Q.; Lifshitz, Y.; Ma, D. D. D.; Zhao, Y. L.; Frauenheim, T.; Lee, S. T.; Tong, S. Y. *J. Chem. Phys.* **2005**, *123*, 144703–144707.
(58) It is reasonable to assume that the supporting Si substrates of the Si NW samples have minor (or no) contribution to the obtained XPS signals. This argument was supported via a series of complementary experiments in which time of flight secondary ion mass spectroscopy (ToF SIMS) depth profiles were obtained for fresh CH_3-Si NW samples. In these experiments (data not shown), sputtering up to 3−4 μm exhibited ToF SIMS values similar to those obtained for non-sputtered C1-Si NW samples. In contrast, sputtering 4−5 μm of the Si NWs layer (i.e., the estimated depth at which the signal from the 2D Si substrate starts to be dominant) exhibited values that are similar to those of the 2D C1-Si(100) surfaces.
(59) Hamad, K. S.; Roth, R.; Rockenberger, J.; van Buuren, T.; Alivisatos, A. P. *Phys. Rev. Lett.* **1999**, *83*, 3474–3477.
(60) Borchert, H.; Talapin, D. V.; McGinley, C.; Adam, S.; Lobo, A.; de Castro, A. R. B.; Moller, T.; Weller, H. *J. Chem. Phys.* **2003**, *119*, 1800–1807.
(61) Iwan, M.; Kunz, C. *Phys. Lett. A* **1977**, *60A*, 345–347.
(62) Dibiase, N.; Gabetta, G.; Lumachi, A.; Scagliotti, M.; Parmigiani, F. *Appl. Phys. Lett.* **1995**, *67*, 2491–2493.
(63) Pasquarello, A.; Hybertsen, M. S.; Car, R. *Phys. Rev. B* **1996**, *53*, 10942–10950.
(64) Tufts, B. J.; Kumar, A.; Bansal, A.; Lewis, N. S. *J. Phys. Chem.* **1992**, *96*, 4581–4592.
(65) Mende, G.; Finster, J.; Flamm, D.; Schulze, D. *Surf. Sci.* **1983**, *128*, 169–175.
(66) Because of shadow effects, the XPS beam reaches only 50−55% of the outer shell of Si NWs grown (and examined) on top of the Si substrate (please note that the penetration depth of the XPS beam in our samples is ~1 nm). Our calculations show that the mentioned 50−55% surface area of Si NW samples is similar to that of 2D Si (100) samples, which are illuminated with the same XPS beam diameter. In other words, the (XPS) energy densities of the Si NW and 2D Si(100) samples are similar to each other.
(67) The peak area at 286.7 eV in C1s, which is ascribed to adventitious carbon bonded to oxygen, was observed equally for all samples (see Supporting Information, Table 1S). This indicates that stabilities of the various samples, as compared to each other, are not from the additional (contamination) adlayer but rather from the monolayer per se.
(68) Raymond, C. *Physical Chemistry*, 3rd ed.; University Science Books: Sausalito, CA, 2000.
(69) Wallart, X.; de Villeneuve, C. H.; Allongue, P. *J. Am. Chem. Soc.* **2005**, *127*, 7871–7878.
(70) Ulman, A. *Chem. Rev.* **1996**, *96*, 1533–1554.
(71) Schwartz, D. K. *Annu. Rev. Phys. Chem.* **2001**, *52*, 107–137.
(72) Schreiber, F. *Prog. Surf. Sci.* **2000**, *65*, 151–256.
(73) Nuzzo, R. G.; Zegarski, B. R.; Dubois, L. H. *J. Am. Chem. Soc.* **1987**, *109*, 733–740.
(74) Nuzzo, R. G.; Fusco, F. A.; Allara, D. L. *J. Am. Chem. Soc.* **1987**, *109*, 2358–2368.
(75) Dubois, L. H.; Nuzzo, R. G. *Annu. Rev. Phys. Chem.* **1992**, *43*, 437–463.
(76) Bain, C. D.; Troughton, E. B.; Tao, Y. T.; Evall, J.; Whitesides, G. M.; Nuzzo, R. G. *J. Am. Chem. Soc.* **1989**, *111*, 321–335.
(77) Bain, C. D.; Whitesides, G. M. *Angew. Chem.* **1989**, *101*, 522–528.
(78) Gorostiza, P.; De Villeneuve, C. H.; Sun, Q. Y.; Sanz, F.; Wallart, X.; Boukherroub, R.; Allongue, P. *J. Phys. Chem. B* **2006**, *110*, 5576–5585.
(79) Wang, D.; Chang, Y.-L.; Liu, Z.; Dai, H. *J. Am. Chem. Soc.* **2005**, *127*, 11871–11875.
(80) Hanrath, T.; Korgel, B. A. *J. Am. Chem. Soc.* **2004**, *126*, 15466–15472.

JP905394W